CFD – facilitated Prognosis of Bubble Bed Bioreactor Performance Based on Bubble Swarms Oscillation Analysis

S. D. Vlaev,[a,*] P. Staykov,[a] and M. Fialova[b]

[a] Institute of Chemical Engineering at the Bulgarian Academy of Sciences,
  Acad. G. Bonchev Str. Bl. 103, 1113 Sofia, Bulgaria

[b] Institute of Chemical Process Fundamentals of the ASCR, v.v.i.,
  Rozvojová 135, 165 02 Prague 6, Czech Republic

Dedicated to the memory of Professor Dr. Valentin Koloini

Bubble column reactors are widely used as gas-liquid and gas liquid-solid contactors in biotechnology applications. A basic issue in biotechnology is oxygen availability related to gas hold-up distribution, since aerobic bioprocessing depends on the dissolved oxygen substrate. The aim of this study is to analyze oxygen availability in bubble column bioreactors in terms of specific spatial and temporal gas-liquid flow. 3D CFD simulation is used to simulate the dispersed gas-liquid flow field of a bubble column of ID 0.29 m equipped with metal distributing plate. The solution is based on the Euler/Euler approach, the standard k-ε model, and the standard wall function treatment. A single size particle model was employed. No mass transfer between the gas and the liquid phase was studied; oxygen transfer is discussed in terms of local and temporal gas hold-up distribution. Two cases of different viscosity are studied related to water-like and sugar-containing nutrient media cases, e.g. tap water and aqueous solution of 0.3 kg kg^{-1} saccharose, respectively. Conditions of oxygen availability for aerobic cell growth in a bio-fluid at condition of elevated viscosity are considered. The time-course of instantaneous oxygen delivery proportional to the dispersion capacity estimated as gas hold-up is uncovered. The results are presented in the form of contour plots and radial profiles of the local gas hold-up at different bed height positions. The oscillating behaviour of the gas hold-up is illustrated and summarized into oxygen availability plot related to position. Based on the CFD analysis, clues for rational bioprocess performance time-course could be inferred.

Key words:
Bubble column bioreactor, gas holdup, CFD simulation

Introduction

Bubble column reactors are widely used as gas-liquid and gas-liquid-solid contactors in biotechnology applications. In such applications, it is important to control the flow field phenomena and substrate delivery including dissolved oxygen using some cheap and straight-forward predictive methodology.[1] Focusing on the diagnostic issues related to the fluctuating bioreactor conditions, one should concentrate on the fluid dynamic impact by following the image of local and instantaneous fluid flow circulation.[2,3] Recent reaction engineering methodology allows generation of such information by computational fluid dynamic (CFD) modeling.

Referring to the literature starting in the late 90s, numerous treatments of bubble column reactor analyses have reported on CFD in bubble columns.[4–8] Reduced to unsteady effects, simulation studies relevant to the unsteady flow topics considered have been reported by several authors.[9-17] A large part of these studies consider gross gas-liquid flow field simulation, while the potentials of using this method for elemental bioreactor analysis have been represented only marginally.

The aim of this study is to generate the unsteady flow behavior of a bubble column bioreactor and to interpret its flow conditions in terms of oxygen availability in bioreactor performance analysis.

Notes on correlations

Referring to the basic relationship of oxygen transfer in aerobic processing,[18] in the cell growth process oxygen transfer rate (OTR)

$$OTR \sim k_L a \, (C^* - C) \tag{1}$$

is counter-balanced by oxygen uptake rate (OUR)

$$OUR \sim (Q_{O_2 max}) \cdot x \tag{2}$$

to yield biomass growth.

* Corresponding author: Tel: +359-2-710 029; E-mail: mixreac@bas.bg

From

$$dC/dt = k_L a \, (C^* - C), \tag{3}$$

oxygen availability can be represented by $k_L a$ that is related to flow conditions, as

$$k_L a = m \, U_G^{\,b} \tag{4}$$

and since $a = 6 \, \varepsilon / d_B$, also as

$$\varepsilon = n \, U_G^{\,b} \tag{5}$$

In biological fluids, due to non-coalescent conditions in the presence of salts and organics, $k_L a$ and ε show similar slope and position, so that the changes in $k_L a$ can be attributed largely to changes in gas hold-up.

On the other hand, oxygen and its availability depend also on the OUR and thus on cell residence time in a zone and on cell metabolism. Related to flow conditions, one can use cell residence time in circulatory structures to predict the cell impact on dissolved oxygen availability. According to the circulation flow model,[19] circulation time can be determined from zone size L proportional to column diameter D_r and liquid circulation velocity u_{Lc}, thus, $t_c = L/u_{Lc}$, where

$$u_{Lc} = \left(\frac{D_r u_{0G} (\rho_L - \rho_G)}{(2.5 \rho_L)} \right)^{1/3}. \tag{6}$$

Consequently, the OUR function is also related to flow.

In order to predict the bubble column bioreactor performance, the following analysis had to be carried out: (1) The flow field of the bubble column is simulated and validated, (2) The circulation patterns and the circulatory structures (vortices, swirls) are traced and the local distribution of gas hold-up and velocities is determined, (3) the specific mass transfer rate ratios and circulation times of the individual structures are determined, (4) the possible implications of the estimated differences in flow capacity to support cell growth and productive reactivity are discussed.

Experimental

Experimental system studied

In view of performing the meshing procedure and for benchmarking the solution, the following experimental background was referred to: a bubble column *ID* 0.29 m, $H = 1.5$ m and clear liquid height $H_0 = 0.9$ m, was employed. The gas distributor comprised a perforated plate with 67 holes of 1.6 mm in diameter, the holes spaced uniformly on the plate area in triangular pitch sided 3.5 cm. The free plate area ratio was 0.2 %. The fluid phases were air and 0.3 kg kg^{-1} saccharose solution in water or air-water for the sake of comparison. The input liquid viscosity of the saccharose solution was 2.7 mPa s. In all experiments, the airflow rate was a moderate one of 10 m^3 h^{-1}, a superficial velocity $u_{0G} = 0.0421$ m s^{-1}. The initial velocity of air in the hole was 21 m s^{-1} and the bubble size diameter was assumed to be 5 mm, as determined by the equation of Lee and Meyrick according to Kastanek *et al.*[19] and compared with reference measurement data.[12] Correspondingly to spatial gas and liquid velocity differences, Reynolds number varied in the range $400 < \text{Re} < 1040$.

Methods employed

The CFD methodology of solving the theoretical model of real gas-liquid flow and post-processing of its solutions was followed. This way direct visualization and mapping of circulatory flow structures were accomplished. The gas-liquid flow model was solved.

The solution was based on the Euler/Euler two-phase modeling approach.[8,20] The mixture turbulence model was used with parameters kinetic energy k and rate of energy dissipation ε' delivered from the relevant transport equations[20] with density and velocity for the mixture.

$$\rho = \rho_m = \sum_{i=1}^{N} \alpha_i \rho_i,$$

$$U_m = \frac{\displaystyle\sum_{i=1}^{N} \alpha_i \rho_i U_i}{\displaystyle\sum_{i=1}^{N} \alpha_i \rho_i}, \text{ as for the single-phase } k\text{-}\varepsilon \text{ model.}$$

By reference to previous analyses of the multiphase model,[12,21] the interfacial momentum transfer M has been reduced to its drag force term

$$M = \frac{3}{4} \rho_L \alpha_G \alpha_L \frac{C_D}{d_B} |U_G - U_L| (U_G - U_L). \tag{7}$$

The drag coefficient C_D was calculated based on Schiller-Nauman model used by default in Fluent:[20]

$$C_D = \frac{24}{\text{Re}} (1 + 0.15 \, \text{Re}^{0.687}), \tag{8}$$

where $\text{Re} = \rho_L d_B (U_G - U_L)/\mu_L$

No mass transfer between the gas and the liquid phase was considered and the dispersed phase

was represented by a single phase with effective bubble diameter (no coalescence or break-up).

Experimental mean and local values of gas hold-up were determined: The local value at various heights was measured by two-plate conductivity probe and the average value was determined by bed expansion.

Simulation details

The geometry and mesh were constructed using the GAMBIT tool of the CFD package FLUENT.[20] The grid consisted of $0.5 \cdot 10^6 - 0.75 \cdot 10^6$ grid cells. There was grid refinement around the holes. Tetrahedral mesh with sizing function vicinity was used to model the nozzles. Boundary layer was used near the walls. Grid independency was checked based on flow field gas and liquid velocity.

Fluent unsteady first-order implicit solver (Fluent Inc., 2003)[20] was used. Pressure-velocity coupling was employed using Phase Coupled – SIMPLE algorithm, as the only possible choice for the pressure-based solver when combined with the Euler-Euler multiphase solution. The integration of the governing equations resulted in a set of linear algebraic equations which were solved by iterative Gauss-Seidel procedure. The standard values for the empirical constants as proposed for single-phase flow, were used. Convergence was checked using 10^{-3} residual monitor value for each variable. The computations were carried out using PC platform operating under Windows. The time step was 0.01 s performing 20 iterations per step. Approximately 20 000 iterations were executed for a 10 s solution. Convergence of a solution took up to 4 days.

The initial and boundary conditions were as follows: The dynamic reactor start-up was followed with the simulation starting at zero gas flow initial condition, i.e. without gas at clear liquid height 0.9 m. Quasi-steady state condition was observed throughout the analysis. At the gas inlet, the inlet velocity for the gas phase with value corresponding to the superficial gas velocity of 4 cm s^{-1}, thus, 21 cm s^{-1} was specified. The liquid volume fraction in the openings was set to zero.[8] No slip conditions were assumed at the column wall. The gas outlet was assumed to vary, the normal liquid velocity and fluxes and the tangential stress being set to zero. The gas outlet was assumed to coincide with the free surface of dispersion and it was set as pressure outlet worth gas volume fraction 1.

The following simulation procedure was followed: (1) Computer generation of the time-course of flow field images and flow patterns, and (2) Post-processing focused on the flow structures – ascending flows, vortices and descending flows.

Results and discussion

Time-averaged flow behavior at quasi-steady state

First, the start-up time was outlined by computing the time-averaged values of total gas hold-up in the column seeking it to be constant. Quasi-steady state for the bioreactor system, i.e. the bubble column filled with saccharose 0.3 kg kg^{-1} and aerated at 10 m^3 h^{-1} (i.e. gas superficial velocity $u_{0G} = 0.0421$ m s^{-1}), was reached following a total performance of up to 20 000 iterations equivalent to reaction time 8 s. For the water-like solution, the steady state condition was obtained in 3 reactive seconds. Following this point, the time-averaged gas hold-up profiles exhibited a constant average value of total gas hold-up of $\varepsilon = 0.155$ for sugar and $\varepsilon = 0.11$ for water. The gas hold-up profiles corresponding to the various column levels in the sugar solution are illustrated in Fig. 1. A part of these profiles was used to match the computed solutions with experimental results for validation. Predicted and measured gas hold-up values in the sugar solution are compared in Fig. 2 and average gas hold-up values are compared in Table 1.
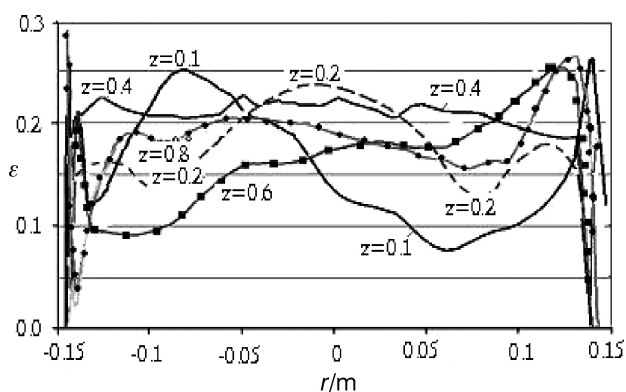

F i g . 1 – *Gas hold-up at various off-bottom levels z (in m) (point symbols serve for curve indication)*
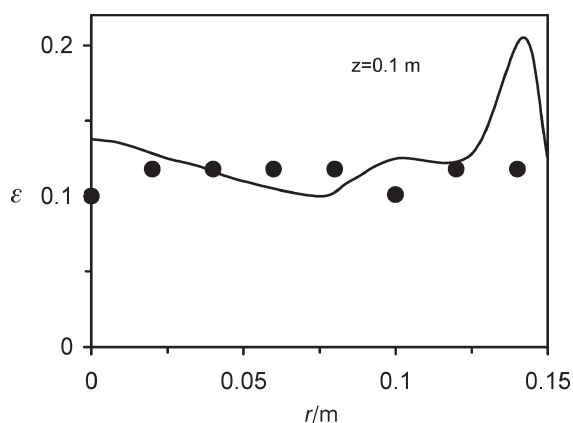

F i g . 2 – *Gas hold-up validation example: predicted (----) vs. measured (●) data*

T a b l e 1 – *Comparison of experimental and predicted gas hold-up values*

Solution	Viscosity/ mPa s	Density/ kg m^{-3}	ε_{exp}	d_B/mm CFD	ε CFD
Saccharose 30 wt %	2.7	1127	0.120	5	0.15
Water	1	998	0.135	5	0.11

* Air flow rate: 10 m^3 h^{-1}, superficial velocity u_{0G} = 0.0421 m s^{-1}, linear velocity of air at the holes = 21 m s^{-1}

Unsteady flow behavior at quasi-steady state

As stated above, in order to predict bioreactor behavior, one should determine local oxygen availability and thus, determine the conditions of the local circulatory flow, e.g. velocity, flow pattern, and calculate the circulation time distribution. Consequently, the instantaneous flow fields of liquid and gas were generated for the case studied.

Partial views containing only the characteristic periodicity of bubble plume oscillation following a small time step of 5 s are shown in Fig. 3. From this and other data (not shown), the plume oscillation time in saccharose solution was determined to be up to 10 s. In general, as reported by various authors,[12,22] bubble swarm rotation in water lasts for as long as 10 s depending on vessel size. The low value obtained in the sucrose case studied was due to the lower viscosity of the liquid and the small size of the vessel (*ID* 0.3 m). At high viscosity and larger vessel, as high as 100 s periodic flows may be registered.

Aimed at the flow field zones indicated in Fig. 3a, the gas/liquid velocity fluctuations (Fig. 4) and void fraction fluctuations (Fig. 5) in the experimental reactor were obtained. The zones poor (P) and rich (R) in oxygen were indicated. Correspondingly to these figures, '*X-Y*' plots of gas hold-up and gas velocity were uncovered and can be shown to illus-
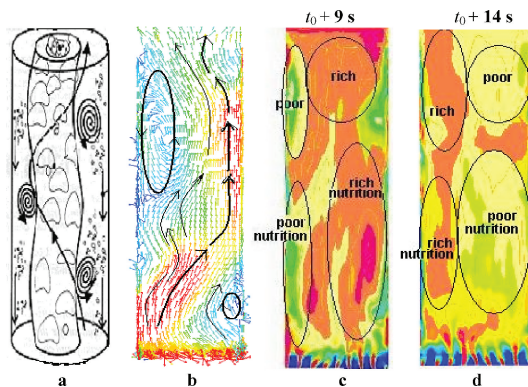
trate the fluctuations of the environment to which cells were exposed. An example is shown in Fig. 6. Bearing in mind the proportionality between gas hold-up and oxygen transfer (eqs. (4), (5)), oxygen availability oscillations represent proportionally the time-fluctuations of gas hold-up.
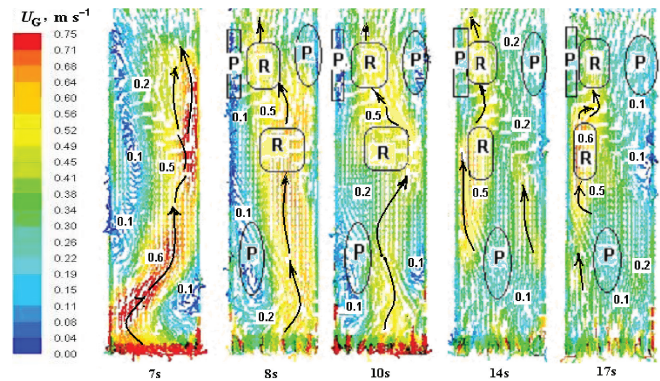

F i g. 4 – *Gas/liquid velocity time-course (pattern, image). The zones of rich (**R**) and poor (**P**) nutrition are indicated.*
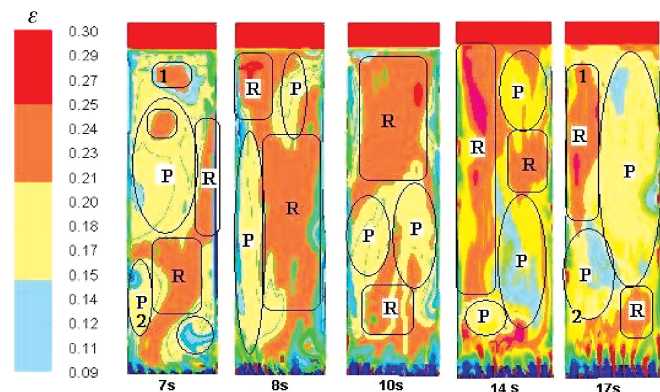

F i g. 5 – *Gas hold-up distribution time-course corresponding to the case of Fig. 4 (Positions 1 and 2 remain unchanged within the time of observation of 10 s)*

F i g. 3 – *Zones of poor (**P**) and rich (**R**) nutrition corresponding to zones of contrasting (high and low) gas hold-up: (**a**) prevailing concept; (**b**) instantaneous gas velocity vector plot yielding the instantaneous gas hold-up distribution contour plot at $t_0 + 9$ s (**c**) followed by instantaneous plot at $t_0 + 14$ s (**d**)*
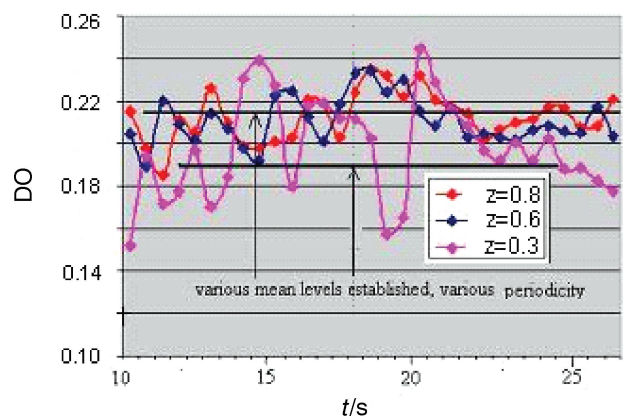

F i g. 6 – *Oscillation of individual parameter (oxygen availability) corresponding to the bubble swarm oscillation dynamics*

According to Figs. 4–5, gas hold-up varied in the range 0.005 to 0.27 and gas linear velocity varied between 0 and 0.7 m s^{-1} yielding values of gas superficial velocity in the range 0 and 0.2 m s^{-1}. It is noteworthy that these values remained stable within the time of plume oscillation, as determined for the specific case above. This time has been found to be comparable with the liquid circulation time relevant to the circulatory structures.

From the gas superficial velocity maximum and minimum values above, the circulation time was determined by eq. (6). It was found that its variations ranged from 3 to 50 s. (Deep analysis may show variations of 100 s for highly viscous nutrient solutions). Such differences of cell residence time should be considered significant to cause changes in cell metabolism.

In order to illustrate the use of the above data for predicting bioreactor performance, the data on oxygen sensitive *Bacillus subtilis* fermentation reported by Amanullah *et al.* (1993)[23] were used. Fig. 7 compares the variation of biomass concentration measured by these authors for the oxygen-sensitive model culture (e.g. the solid line) and the variation corresponding to the specific flow conditions of this study (the points). It can be seen that the change in cell circulation time between 3 and 44 s predicted in this study would bring up to 30 % deviation in biomass growth. This result supports the potentials of the suggested prognostic procedure.
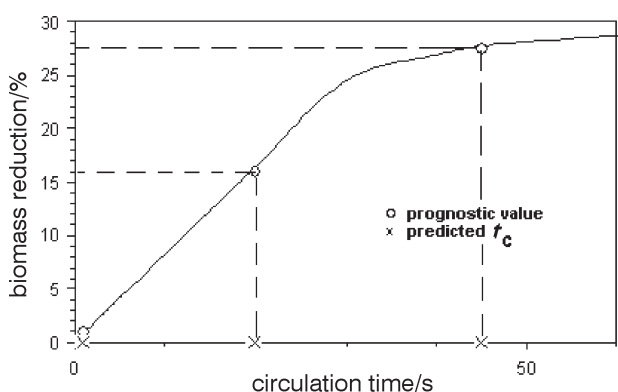

F i g . 7 – *Predicted behavior based on the flow conditions in the bioreactor of this study (i.e. the x-points circulation time t_c) versus reference data – the line (Amanullah et al., 1993)[23] on biomass reduction for an oxygen-sensitive model microorganism (B. subtilis)*

To summarize, a procedure of bubble column flow analysis application to bioprocess analysis in terms of substrate/oxygen availability is proposed. According to this procedure, the CFD-generated unsteady oscillatory flow is being mapped and correlated with oxygen availability and the extremes of the substrate-rich and substrate-poor zone characteristics (namely, velocities, circulation times) are determined and compared. Combining these data with the dynamic characteristics of an oxygen-sensitive model culture (e.g. reference data on *Bacillus subtilis* fermentation time course), the limits of bioreactor performance parameters, such as biomass or product concentration can be assessed.

Conclusion

Conditions of oxygen availability for aerobic cell growth in a bio-fluid containing sucrose where viscosity is elevated have been analyzed: The time-course of instantaneous oxygen delivery is related to dispersion capacity estimated as gas hold-up. The latter is evaluated by simulation of "real" gas-liquid flow via the Euler-Euler and RANS modeling schemes. Following flow simulation of the flow regimes referred mainly to highly viscous nutrient media, the differences in gas (air) hold-up and cell residence – in substrate-rich and substrate-poor circulatory structures – are demonstrated to be large enough to result in failures of cell growth. In view of improving bioreactor production yields, CFD methodology can be successfully employed to predict pathological conditions in nutrient media of bubble column bioreactors.

List of symbols

a – gas-liquid interfacial area per unit volume of liquid area, m^{-1}

b – exponent in eq. (4) and eq. (5)

C – dissolved oxygen concentration in the liquid phase, mmol m^{-3}

C^* – dissolved oxygen concentration at air saturation, mmol m^{-3}

C_D – drag coefficient

d_B – bubble diameter, m

D_r – column diameter, m

DO – dissolved oxygen saturation

H – height of column, m

H_0 – clear liquid height, m

k – turbulent kinetic energy, m^2 s^{-2}

$k_L a$ – volumetric mass transfer coefficient, s^{-1}

L – zone size, m

m – constant in eq. (4), m^{-b} s^{b-1}

M – momentum inter-phase exchange term, kg m^{-3} s^{-1}

n – constant in eq. (5), s^b m^{-b}

$Q_{O_2\ max}$ – maximum specific oxygen uptake rate, mmol kg^{-1} biomass s^{-1}

r – radial distance, m

U – mean velocity of phase, m s^{-1}

u_{0G} – superficial gas velocity, m s^{-1}

u_{Lc} – liquid circulation velocity, m s^{-1}

t_0 – zero time of no change of input variables, s

t_c – circulation time, s

x – biomass concentration, kg m^{-3}

z – axial distance, m

Greek letters

α – volume fraction of phase

ε – gas holdup

ε' – rate of energy dissipation, m^2 s^{-3}

μ – dynamic viscosity, Pa s

ρ – density, kg m^{-3}

Subscripts

I – phase (gas or liquid)

G – gas

L – liquid

m – mixture

References

1. *Berovic, M., Koloini, T.*, Bioreactor Engineering Course. Boris Kidrič Institut of Chemistry, Ljubljana, 1991.

2. *Milavec Žmak, P., Podgornik, A., Podgornik, H., Koloini, T.,* In: *Avsic-Županc, T.* (Ed.). 1st FEMS Congress of European Microbiologists (Slovenia, Ljubljana, June 29 – July 3, 2003) Abstract book, FEMS, Delft, 2003, pp 14-24.

3. *Kurtanjek, Z.,* Current Studies of Biotechnology **2** (2001) 89.

4. *Delnoij, E., Kuipers, J. A. M., van Swaaij, W. P. M.*, Chem. Eng. Sci. **52** (1997) 3623.

5. *Sundaresan, S.,* AIChE J. **46** (2000) 1102.

6. *Joshi, J. B.*, Chem. Eng. Sci. **56** (2001) 5893.

7. *Pfleger, D., Becker, S.,* Chem. Eng. Sci. **56** (2001) 1737.

8. *Ranade, V. V.,* Computational Flow Modeling for Chemical Reactor Engineering, Academic Press, San Diego, 2002.

9. *Kurtanjek, Z.*, Chem. Intell. Lab. Systems **46** (1999) 149.

10. *Bernard, S. R., Maier, R. S., Falvey, H. T.*, Applied Mathematical Modelling **24** (2000) 215.

11. *Bertola, F., Vanni, M., Baldi, G.*, International Journal of Chemical Reactor Engineering **1** (2003) A3.

12. *Buwa, V. V., Ranade, V. V.*, Can. J. Chem. Eng. **81** (2003) 411.

13. *Davidson, K. M., Sushil, Sh., Eggleton, Ch., Marten, M.*, Biotechnol. Prog. **19** (2003) 1480.

14. *Wiemann, D., Mewes, D.,* Chem. Eng. Sci. **60** (2005) 6065.

15. *Fayolle, M., Cocks, A., Gillot, S., Roustan, M., Héduit, A.*, Chem. Eng. Sci. **62** (2007) 7163.

16. *Irani, M., Bozorgmehri, M.*, Proc. 17th International Congress of Chemical and Process Engineering CHISA (Prague, 27-31 August 2006) Summaries 3, Prague, 2006, pp 704-705.

17. *Dhotre, M. T., Smith, B. L.*, Chem. Eng. Sci. **62** (2007) 6615.

18. *Atkinson, B., Mavituna, F.*, Biochemical Engineering and Biotechnology Handbook, Nature press, New York, 1983, pp 727, 791-795.

19. *Kastanek, F., Zahradnik, J., Kratochvil, J., Cermak, J.*, Chemical Reactors for Gas-Liquid Systems, Ellis Horwood, New York, 1993, pp 215-219.

20. Fluent Inc, 2003, Fluent 6.1 Documentation, CD-ROM, New Hampshire, USA.

21. *Tomiyama, A., Tamaia, H., Zun, I., Hosokawa, S.*, Chem. Eng. Sci. **57** (2002) 1849.

22. *Lehr, F., Millies, M., Mewes, D.*, AIChE J. **48** (2002) 2426.

23. *Amanullah, A., Nienow, A. W., Emery, A. N., McFarlane, C. M.,* Trans IChemE **71**(C) (1993) 206.